

ELECTRON EMISSION IN RELATIVISTIC LASER-DROPLET INTERACTIONS

L. Di Lucchio, P. Gibbon

Forschungszentrum Jülich GmbH, Institute for Advanced Simulation, Jülich Supercomputing Centre, D-52425 Jülich, Germany

Ultrashort electron bunches created by the interaction of high-intensity, femtosecond laser pulses with plasma targets can be utilised as a powerful source of attosecond X-ray pulses. The latter can be produced by bombarding a secondary target with such electron bunches and have an immediate application in X-ray microscopy and ultrafast atomic dynamics studies. Recently, the generation of efficient attosecond bunches production by laser-illuminated droplets has become feasible due to the availability of both ultraintense and ultrashort laser pulses and of stabilised nanometer-sized droplet targetry at a number of laboratories.

In this work we analyze in detail the mechanism of efficient generation of ultrashort dense electron bunches from the surface of a small droplet illuminated by a two-cycle (fwhm = 5 fs) ultraintense Gaussian laser pulse. In contrast to previous work in Ref.^[1], our spherical nanotargets have a solid-like density of $n = 100n_c$, where $n_c = 1.8 \times 10^{21} \text{ cm}^{-3}$ is the critical density. Clusters with a range of sizes have been considered, starting with a much smaller radius than the laser focus, namely of 100-200 nm, comparing their dynamics with clusters up to a 1 micron radius, that is, a size comparable to the focus. The intensity of the laser was varied between $10^{17} - 10^{21} \text{ Wcm}^{-2}$ to determine scaling behaviour for the emitted particles' energies and emission angles. Our simulations have been performed with the particle-in-cell code EPOCH. The simulation box size was varied between 4 and $20 \mu\text{m}$, while the cell size was maintained at $\approx 8 \text{ nm}$. The number of simulation particles was 34×10^6 ions and electrons.

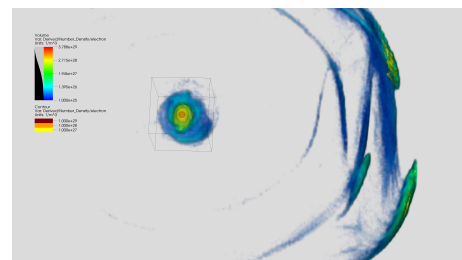


Figure 1: 3D electron density plot of a 100nm size droplet illuminated by a 2-cycle pulse at $I=10^{20} \text{ W/cm}^2$. The bunches are represented by the counted regions.

A number of 3D simulations were made to test the dynamics of the electrons at early times. The bunches are emitted as every half-cycle of the laser pulse strikes the droplet, as foreseen in Ref.^[1]. For smaller droplets, i.e. 100 nm size, the emitted bunches form narrow optically overdense regions travelling together with the pulse at the rear side of the cluster, and tend to place themselves on the same plane as the incident wave already a few femtoseconds after

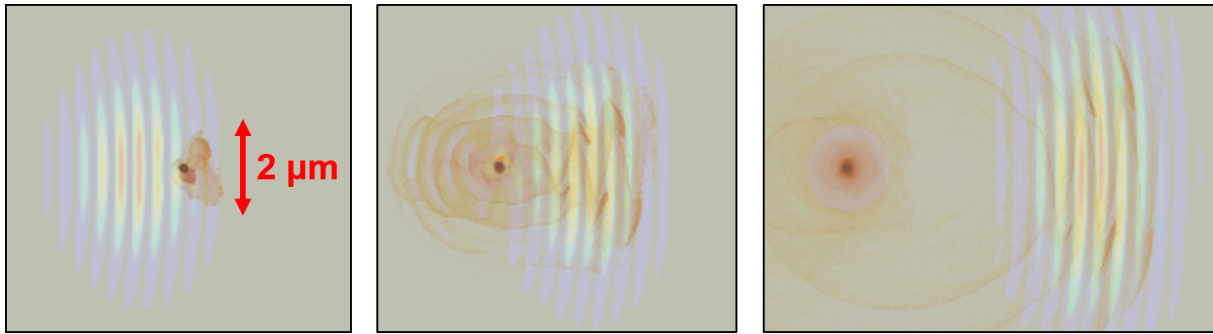


Figure 2: 2D plot of electron density plots superimposed with laser energy density, just before, during and soon after the interaction for a 100nm size droplet illuminated by a 2-cycle pulse at $I=10^{20}\text{W}/\text{cm}^2$

the interaction (fig. 1). However, contrary to Ref. [1] at relativistic laser intensities, simulation results do not agree with Mie scattering patterns for droplets whose radius is lower than $\lambda/2$. For such droplets, the inclination of the bunches appears to be deviated as soon as they leave the surface, with an angle which depends on the size of the droplet and the intensity of the laser. Since 3D simulations at such a high density as $100n_c$ are computationally expensive, we have performed 2D simulations in the plane of the electromagnetic wave where the most of the dynamics at later times ($\approx 100 - 200$ fs) effectively occurs. These simulations show that the electron bunches – which in this case are overdense – continue to interact with the laser pulse after the emission – Fig. 2.

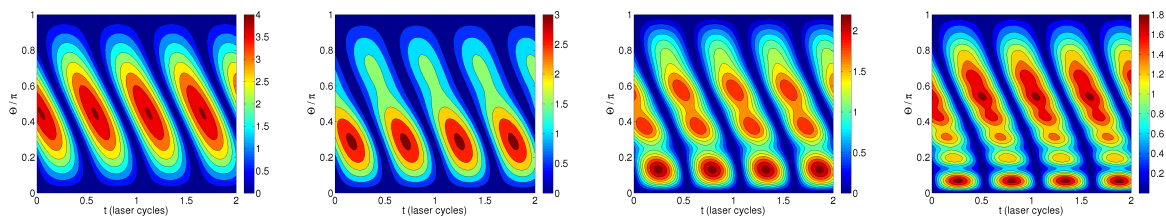
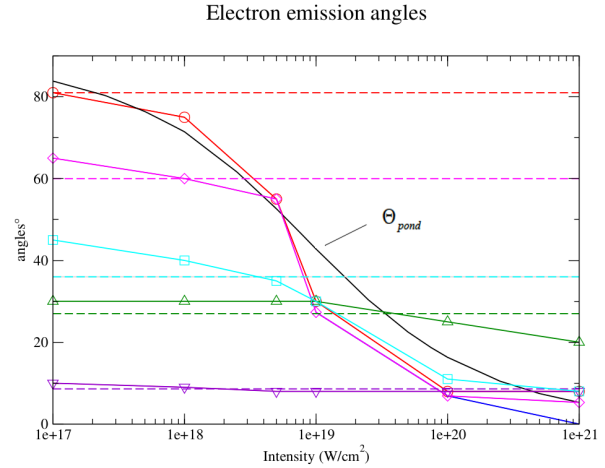


Figure 3: Enhancement of absolute radial electric field as a function of the incident electric field E_0 for a $100 n_c$ droplet with $R=100\text{nm}$ (a), 200nm (b), 500nm (c) and 1micron (d) in an incident plane wave of constant amplitude and wavelength $\lambda = 800\text{nm}$ as a function of time and angle on the surface.

The Mie scattering patterns for small droplets are computed assuming a linear dielectric constant in the plasma region and so cannot account for any intensity-dependant behaviour in the bunch emission – see fig. 3. Moreover, Mie theory is based on the assumption that $R \gg \delta$, where R is the droplet radius and $\delta = c/\omega_p$ is the plasma skin depth. This condition can be fully satisfied for droplets whose size is comparable or bigger than the laser focus, and in this case a fair agreement is found between simulation results and Mie scattering predictions. By contrast, simulations for 100-200nm droplets show a strong deviation from Mie theory predictions – Fig.4 – suggesting that this condition needs to be modified to $R \sim \delta_r$, where $\delta_r = \gamma^{1/2}\delta$ is

Figure 4: *Electron emission angles as a function of laser intensity and droplet size (red = 100nm, magenta= 200 nm, cyan= 300nm, green=500nm, violet=1 μ m), compared with models discussed in the text. Solid lines represent simulation points, dashed horizontal lines the Mie theory prediction. Black and blue lines represent predictions of Eq.1 and Eq.2, respectively.*



the effective skin depth taking into account the induced transparency effect which occurs for relativistic intensities. The effective plasma frequency is $\omega_p^r = \omega_p/\gamma^{1/2}$ and therefore for $\gamma = \sqrt{1 + a_0^2} \approx 5 - 20$, we have $\delta_r \approx 40 - 60nm$, which is of the same order as R for the smaller droplets. In this case it makes more sense to apply a relativistic interaction model such as the ponderomotive scattering of electrons by an intense field at laser focus^[3].

The scattering angle of a single electron in the laser focus in vacuum is given by

$$\theta_0 = \arctan \frac{\sqrt{\frac{2}{1+\beta_0} \left(\frac{\gamma}{\gamma_0} - 1 \right)}}{\gamma - \gamma_0(1 - \beta_0)}, \quad (1)$$

where γ_0 and β_0 are the initial energy and normalised transverse momentum of the particle, respectively. For an electron initially at the rest on the droplet surface, $\gamma_0 = 1$ and $\beta_0 = 1$, in which case Eq.1 reduces to $\theta_0 = \arctan \sqrt{2/(\gamma - 1)}$, as displayed by the black curve in Fig.4.

As soon as the bunches leave the droplet they are exposed to the field of the scattered laser pulse, in a similar manner to electrons driven by a short laser pulse reflected from a finite-sized plane target, as described in Ref. ([4]). In the case of small droplets with $R < \lambda/2$ most of the pulse is actually transmitted, so that the highest field gradients are in the rear side vacuum region, where also most of the electrons are expelled. The electron bunches have high ($n_b > n_{cr}$), implying that they will still be subject to ponderomotive while sitting between phases of the laser field. During the co-propagation with the laser pulse they lose part of their longitudinal momentum and of their density, thus lowering their inclination.

In Ref^[4] this effect is related to the characteristic parameters of the bunches, namely the number of particles N_b they contain and their longitudinal thickness d_b . As long as the electrons kinetic energy overcomes the electrostatic potential energy of the bunch (Coulomb barrier threshold), that is, $N_b \epsilon_e > e^2 N_b^2 / d_b$, the normal component of the momentum is progressively

reduced by an amount corresponding to the space-charge force contribution from the ionized droplet. For a 100nm droplet and a laser intensity $I = 10^{19} \text{ Wcm}^{-2}$ one can estimate $N_b \approx 10^8$ and $d_b \approx 100 \text{ nm}$ (corresponding to a duration of 300 attoseconds) from the simulations, and the corresponding threshold energy of 1.4 MeV is easily overcome. Defining $p_{\perp} = p_y \sin \theta$ and $p_{\parallel} = p_x \sin \theta$ as the components of the momentum along the perpendicular and tangential directions with respect to the droplet surface (see Fig. 5), these are modified by the space charge via the relations: $p'_{\perp} \approx p_{\perp} - e^2 N_{bm} / cd_m$; $p'_{\perp} = p'_y \sin \theta'$; $p'_{\parallel} = p'_x \sin \theta' = p_{\parallel}$, giving a final emission angle varies according to $\theta' = \arctan(p'_y / p'_x)$.

In conclusion, droplets with $R < \lambda/2$ emit electron bunches at angles differing significantly from values expected from linear Mie theory, following instead trajectories which deflect towards the laser axis in the relativistic regime through a combination of ponderomotive scattering and space-charge deflection after emission. This transition from the Mie-scattering-dominated and the relativistic nanodroplet regime is fully summarized in Fig. 4.

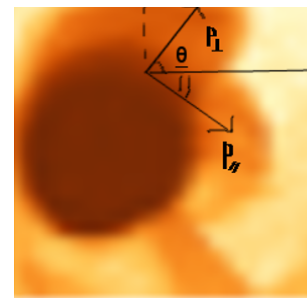


Figure 5: *Geometry of bunch deflection due to space charge*

Acknowledgements

The authors acknowledge computing resources under grant VSR-JZAM04 and thank Dr. H Zilken and the visualization team of the Jülich Supercomputing Centre, for assistance with the rendering for the 3D simulations.

References

- [1] T.V. Liseykina, S.Pirner, D.Bauer, Relativistic Attosecond Bunches from Laser-Illuminated Droplets, PRL **22**, 2010.
- [2] P.W.Barber, S.C.Hill, Light Scattering by Particles:Computational Methods, World Scientific, Singapore, 1990.
- [3] F.V.Hartemann et al, Nonlinear ponderomotive scattering of relativistic electrons by an intense laser field at focus, Phys. Rev. E, 1995.
- [4] A.A.Andreev, K.Y.Platonov, Generation of electron nanobunches and short-wavelength radiation upon reflection of a relativistic intensity laser pulse from a finite-size target, Optics and Spectroscopy, 2013, Springer